

abbreviated notation $MM'N$ with the chemical symbol for the elements M and M' .

²J. W. Culvahouse and David P. Schinke, *Phys. Rev.* **187**, 671 (1969).

³J. S. Griffith, *The Theory of Transition Metal Ions* (Cambridge U.P., London, 1961), pp. 347-348.

⁴This result follows from a discussion of exchange interaction in the excellent review by J. Owen and J. H. M. Thornley, *Rept. Progr. Phys.* **29**, 675 (1966). Because of the isotropic exchange between the ionic spins of Co^{2+} we assume that f_{π}^2 is negligible.

⁵Equation (61) of Ref. 2 is used in the calculation of this result. The numerical factor 0.94 in that equation should be 0.97.

⁶K. W. Mess, E. Lagendijk, N. J. Zimmerman, A. J. Van Duyneveldt, J. J. Giesen, and W. J. Huiskamp, *Physica* **43**, 165 (1969).

⁷J. W. Culvahouse, *J. Chem. Phys.* **36**, 1710 (1962).

⁸H. Fenichel and G. Unrine (private communication).

⁹D. K. Brice, doctoral dissertation, University of Kansas, 1962 (unpublished).

¹⁰I. Dzyaloshinski, *Phys. Chem. Solids* **4**, 241 (1958); T. Moriya, *Phys. Rev.* **117**, 635 (1960).

¹¹J. H. Van Vleck, *Phys. Rev.* **52**, 1178 (1937).

¹²Toru Moriya, in *Magnetism*, edited by George T. Rado and Harry Suhl (Academic, New York, 1963), Vol. I, pp. 92ff.

¹³P. W. Anderson, in Ref. 12, p. 41.

¹⁴Junjiro Kanamori, in Ref. 12, pp. 161-164.

¹⁵See Ref. 2, Eq. (27).

¹⁶J. H. Van Vleck, *Phys. Rev.* **74**, 1168 (1948).

¹⁷R. T. Dixon, doctoral dissertation, University of Kansas, 1970 (unpublished).

¹⁸P. W. Anderson, in Ref. 12, p. 67.

¹⁹A. Simon, M. E. Rose, and J. M. Jauch, *Phys. Rev.* **84**, 1155 (1951).

Electron States in Ferromagnetic Iron. II. Wave-Function Properties*

K. J. Duff

*Theoretical Sciences Department, Scientific Research Staff,
Ford Motor Company, Dearborn, Michigan 48121*

and

T. P. Das

*Physics Department, University of Utah, Salt Lake City, Utah 94112
(Received 7 August 1970)*

The wave functions produced by a new band calculation for ferromagnetic iron are examined by computing from them charge and spin densities both at the nuclear position and at other positions throughout the unit cell. Excellent agreement is achieved between the measurable experimental and theoretical quantities, namely, charge and spin densities, the isomer shift, and the hyperfine field. It is shown that the earlier interpretation of neutron-diffraction data and the pressure dependence of the hyperfine field in favor of a negative polarization of the $4s$ states is not soundly based. From our consideration of the band contribution to the hyperfine field, the $4s$ electrons are found to be positively polarized.

I. INTRODUCTION

It is unquestioned that the ferromagnetism of transition metals reflects an unequal spin population of the bands derived from atomic $3d$ states. Naively, one would expect that the bands derived from atomic $4s$ states would be polarized by the exchange interaction with the d states to give a net $4s$ moment parallel to the $3d$ moment. To this simple picture we have to add the effects of hybridization of s and d states which add an antiparallel component of polarization to the s bands,¹ and the resulting moment can be either positively (parallel) or negatively (antiparallel) polarized. Experimentally, evidence has been found that has been interpreted to mean that the $4s$ states of iron, cobalt, and nickel are actually polarized negatively.²⁻⁴ In this paper we consider the properties of the wave functions of conduction electrons in ferromagnetic

iron as derived in a new band-structure calculation described in a previous paper,⁵ with particular emphasis on magnetic properties. We reexamine the question of the polarization of the $4s$ electrons and conclude that they are positively polarized.

The evidence cited for negative polarization is threefold: (a) the angular distribution for the scattering of polarized neutrons²; (b) the pressure dependence of the hyperfine field³; (c) the angular correlation of γ rays from the annihilation of polarized positrons.⁴ We do not consider here (c); however, the interpretation of the positron-annihilation experiments in favor of a negative $4s$ polarization has largely been discredited⁶; it is accepted that for some momenta there is a negative polarization in iron and nickel, but it has not been possible, so far, to derive a net polarization integrated over all momenta.⁷

We must emphasize at this point that we do not

challenge the veracity of any experimental data, but only the interpretation of the data. Thus in Secs. III and V we use the experimental results for the spatial distribution of spin and for the x-ray scattering form factors as a gauge of the accuracy of our wave functions. We find excellent agreement between our calculated quantities and the experimental results. Then with confidence in our wave functions we use them to examine (in Sec. V) the fundamental assumption used in the interpretation of the neutron-diffraction data, that of a crystal-field model, and show that such an assumption does not have validity for the band-*d* electrons of iron.

Anderson³ has examined the pressure dependence of the hyperfine field and the spin per atom for iron, cobalt, and nickel. When pressure is applied, the hyperfine field per spin in each case becomes more negative. In iron this occurs in spite of the fact that the change in total hyperfine field is positive with increasing pressure. Hence, we must distinguish two effects, the first, a change in Fermi-surface geometry which allows a redistribution of population of the magnetic electron states, and the second, a change in contribution per occupied state. We are concerned here with the second effect. Anderson reasons that pressure will have little effect on fairly compact 3*d* wave functions, and so the exchange-induced core polarization (ECP) contribution per spin is unlikely to change significantly with pressure, whereas the density at the nucleus for the 4s wave functions will be almost proportional to the volume changes of the whole solid.⁸ Since an increase in pressure increases the magnitude of the contribution per spin from the 4s states, he therefore concluded that the 4s states give a negative contribution to the hyperfine field, and this in turn suggests a negative polarization of the 4s states. In Sec. VI, we calculate the various contributions to the hyperfine field and again are able to get good agreement with experiment. We find the band contribution to be positive, implying positive 4s polarization, and show that Anderson's assumption of a constant core contribution per spin is suspect.

In Sec. II, we review briefly the method used for the band-structure calculation. The isomer shift is treated in Sec. IV. Section VII is a summarizing discussion.

II. REVIEW OF BAND-STRUCTURE METHODOLOGY

The wave functions used for the calculations reported here were found by a method described in I. Conduction-electron states generically related to atomic 3*d* and 4s states were described by wave functions

$$\psi = \sum_{m=1}^5 \lambda_m u_d^m + \sum_{i=1}^{19} \mu_i u_{\text{OPW}}^i, \quad (2.1)$$

where λ_m and μ_i are variationally derived expansion coefficients, the u_d^m are tight-binding wave functions formed from atomic *d* states, and u_{OPW}^i are orthogonalized plane waves (OPW). The OPW expansion goes to second nearest neighbors in reciprocal-lattice space. The form (1) has sufficient flexibility to describe both diffuse *s* states ($\lambda_m = 0$, $\mu_i \neq 0$), compact *d* states ($\lambda_m \neq 0$, μ_i small), and any hybrid of these. The radial dependence of *d* states is not limited to that of the tight-binding functions used in the expansion since the plane-wave parts of the OPW can contribute $l=2$ character, and thus spin densities can be meaningfully calculated.

Matrix elements of the Hartree-Fock Hamiltonian were computed from (2.1) using a variety of numerical techniques. Exchange matrix elements were computed directly without making a local approximation. Corrections for correlation effects were included by use of the "Coulomb hole plus screened exchange" formalism⁹ for *s*-like states, and an effective exchange formula¹⁰ due to Hubbard for the *d*-like states.

Wave functions and energies were computed at 110 inequivalent points in $\frac{1}{48}$ of the Brillouin zone (BZ). For the results reported below, contributions from each point were totaled using weighting factors assigned on the basis of volume elements of the BZ associated with the points, and on populations of the various states at the points. Two complete calculations were made, corresponding to magnetic moments of 2.06 and 2.19 μ_B /atom.

III. CHARGE DENSITIES AND X-RAY SCATTERING FORM FACTORS

As a first test of the merit of the band wave functions, charge densities were calculated from them, and the charge densities were then Fourier analyzed to give the x-ray scattering form factors. The resulting form factors for the band structure when magnetic moment is 2.19 μ_B /atom are listed in Table I along with the form factors calculated by Wakoh and Yamashita¹¹ (WY), and experimental form factors.^{12,13} The slight difference between the core contribution listed here and those listed by WY are due to different wave functions being used for the core states.

It is seen that considerably better agreement with the experimental form factors is obtained by the present calculation than that of WY, their results being consistently higher than the form factors calculated here, implying a more localized charge density than ours. The band contribution is only a small proportion of the total form factor, and the core contribution is very accurately known. Any discrepancy between the calculated total form factor and the experimental one reflects an inaccuracy in the band wave functions. In WY's calculation, the discrepancy is large, compared with the band

TABLE I. X-ray scattering form factors. The second set of experimental results listed here have been artificially scaled so that the (2, 1, 1) form factor agrees exactly with the first set; this was done because the author of the second set was not able to calibrate his form factors in an absolute sense.

Scattering vector	Core contribution	Band contribution	Total for this calculation	Experiment (Ref. 12)	Experiment (Ref. 13)	Wakoh and Yamashita (Ref. 11)
(1, 1, 0)	15.152	2.438	17.59	17.63 ± 0.20	17.40	18.55
(2, 0, 0)	13.149	1.129	14.28	14.70 ± 0.23	14.24	14.89
(2, 1, 1)	11.700	0.853	12.55	12.62 ± 0.21	12.62	13.01
(2, 2, 0)	10.626	0.627	11.25	11.13 ± 0.20	11.09	11.65
(3, 1, 0)	9.812	0.536	10.35	10.10 ± 0.19		10.53
(2, 2, 2)	9.182	0.384	9.57	9.13 ± 0.25		9.65
(3, 2, 1)	8.685	0.156	8.84	8.75 ± 0.19		8.94
(4, 0, 0)	8.286	0.008	8.29			8.40
(3, 3, 0)	7.958	0.038	8.00	7.68 ± 0.21		8.03
(4, 1, 1)	7.958	-0.014	7.94	7.68 ± 0.21		8.02

contribution, so they were somewhat dissatisfied with their results.

It is important to identify the procedural element in the present calculation which has led to the improved result. The dominant differences between the two calculations are the respective analytic forms of the wave functions and the treatments of correlation and exchange. It is at first tempting to assume that the problem in the calculation by WY centers on the difficulty of describing *d*-state wave functions which are localized and directional with a sum of plane waves in some region, i.e., between muffin tins. However, this does not seem a likely explanation because, if it were true, their energy-band calculation would have suffered from convergence difficulties. In addition, the *d*-spin density calculated in the present work can only be produced by the OPW components of the *d*-state wave functions, so that the accuracy of the *d*-spin density distribution discussed in Sec. V reveals the adequacy of a plane-wave expansion for the calculation of charge densities in the outer regions of an atomic cell.

A recent OPW calculation¹⁴ of charge densities in Si, Ge, and ZnSe, employing up to 230 plane waves, produced well-converged energies and charge densities which were in qualitative agreement with experiment, but which lacked quantitative precision. The authors attributed the deficiency to the inadequacy of the local exchange-correlation potential because this was the only significant approximate feature of an otherwise high precision calculation. A similar conclusion was reached by Arlinghaus¹⁵ by consideration of the charge densities for copper produced by his APW calculation using the $\rho^{1/3}$ exchange. The exchange potential used by WY was also of this form, whereas, for the present calculation, the nonlocal Hartree-Fock exchange was used and corrections for correlation effects were incorporated. It seems clear, then, that this more realistic treatment of exchange and correlation is the decisive factor in

improving the accuracy of the calculation of the charge distribution.

Figure 1 depicts the computed charge densities in the [100], [110], and [111] directions.

IV. ISOMER SHIFT

The isomer shift ϵ is measured in Mössbauer experiments and is linearly related to the charge density of the extra-nuclear electrons at the nucleus undergoing the transition

$$\epsilon = \alpha |\psi(0)|^2 + \text{const.} \quad (4.1)$$

The α is a calibration constant for the particular nucleus, which is related to the change in nuclear radius during the transition and which may be determined by measurements of the isomer shift for two chemical species for which the magnitudes of $|\psi(0)|^2$ can be calculated with good accuracy. That is, the quantities of interest are

$$\epsilon_1 - \epsilon_2 = \alpha [|\psi_1(0)|^2 - |\psi_2(0)|^2]. \quad (4.2)$$

Before discussing our band contribution to the

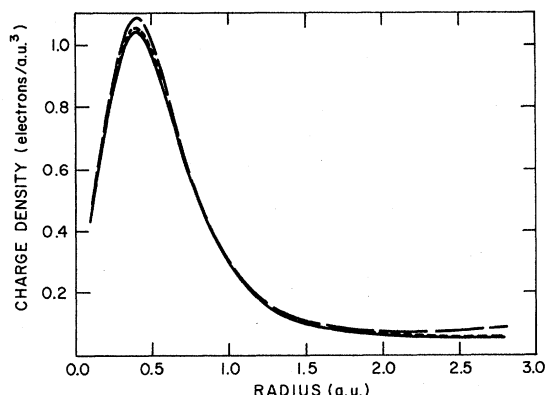


FIG. 1. The radial distribution of charge density deduced from the band wave functions. The solid line, dotted line, and dashed line are for the [100], [110], and [111] directions, respectively.

isomer shift, we will briefly review the experimental and theoretical situation, principally as discussed by Ingalls¹⁶ and Drickamer, Vaughan, and Champion.¹⁷ For the Fe⁵⁷ nucleus, α has been deduced¹⁸ from (4.2) by measurements on ferrous- and ferric-iron compounds, coupled with wave functions taken from free-ion calculations.¹⁹ The value so deduced is $\alpha = 0.47 \pm 0.05 a_0^3$ mm/sec. On this picture the difference $|\psi(0)|^2$ between the ferrous and ferric states is entirely due to greater shielding of the 3s electrons by the additional 3d electron in Fe²⁺.

The use of free-ion wave functions has been called in question by a number of authors.²⁰⁻²² Gol'danski²⁰ and Danon²¹ both argue on the basis of other physical evidence (x-ray absorption spectra, optical data, electronegativity, and molecular-orbital calculations) that, whereas the free-ion picture has substantial validity for Fe²⁺, covalency in Fe³⁺ produces charge transfer to the iron site of both 4s and 3d electrons. The 4s charge density, which is estimated to represent from 0.32 (Ref. 21) to 1.25 (Ref. 20) electrons, contributes directly to $|\psi(0)|^2$, while the additional 3d density acts to screen the 3s density, reducing $|\psi(0)|^2$. Although the authors do not agree on the equivalent configuration for Fe³⁺, they both predict a value for the calibration constant of about $-0.2 a_0^3$ mm/sec. A second suggestion by Simanek and Sroubek²² is that a significant contribution to $|\psi(0)|^2$ can come from distortion of core orbitals due to overlap of ligand orbitals. These authors find $\alpha = -0.16 a_0^3$ mm/sec.

Ingalls¹⁶ has recently studied the isomer shift in a number of situations where both states occurring in (4.2) refer to metallic iron (pressure dependence of the isomer shift, Curie point anomaly, phase transitions), and he finds that better agreement with experiment is obtained by choosing $\alpha = -0.37 a_0^3$ mm/sec. The use of two metallic iron states should be favorable for the cancellation of systematic error in the calculated charge densities, because, if

TABLE II. Charge and spin densities and hyperfine fields at nuclear sites calculated from two sets of band wave functions. For the first set of results the band magnetic moment was $2.06 \mu_B$ /atom, while for the second it was $2.19 \mu_B$ /atom. Majority spin is indicated by †.

	Magnetic moment $= 2.06 \mu_B$ /atom (a_0^{-3})	Magnetic moment $= 2.19 \mu_B$ /atom (a_0^{-3})
$ \psi_{\downarrow}(0) ^2$	2.421	2.441
$ \psi_{\uparrow}(0) ^2$	2.311	2.378
$ \psi_{\downarrow}(0) ^2 + \psi_{\uparrow}(0) ^2$	4.732	4.819
$ \psi_{\downarrow}(0) ^2 - \psi_{\uparrow}(0) ^2$	0.110	0.063
Hyperfine field (kG)	57.7	33.1

errors are made in the potentials, they should be similar for the two states. The pressure experiments have been repeated with greater accuracy by Moyzis and Drickamer²³ and they conclude that $-\alpha$ should not be less than $0.28 a_0^3$ mm/sec, and if Ingalls's assumptions are made concerning s-to-d transfer with pressure, then Ingalls's value of α is reproduced.

From our band wave functions we can compute directly the conduction-electron contribution to $|\psi(0)|^2$, and this is listed in Table II. Although we do not calculate a self-consistent contribution from the core electrons, we note that the 3s charge density ($134.00 a_0^3$) from the $3d^7 4s$ atomic configuration used as a starting point for the band calculation, is almost the same as that assumed by Ingalls from his band calculation. However, our band contribution of $4.82 a_0^3$ is somewhat higher than his. Since we calculated band wave functions for only one lattice spacing and lattice structure, we are obliged to use a free-ion state as the second state when applying (4.2). Using Ingalls's values of charge densities for all but the band charge-density contribution, for which we use our own result, together with experimental values of the isomer shift, we obtain

$$\alpha = \frac{\epsilon(\text{Fe}^{2+}) - \epsilon(\text{Fe})}{|\psi_{2+}(0)|^2 - |\psi_{\text{Fe}}(0)|^2} = -0.32 a_0^3 \text{ mm/sec} \quad (4.3)$$

and

$$\alpha = \frac{\epsilon(\text{Fe}^{3+}) - \epsilon(\text{Fe})}{|\psi_{3+}(0)|^2 - |\psi_{\text{Fe}}(0)|^2} = -0.18 a_0^3 \text{ mm/sec} \quad (4.4)$$

We note that α derived from (4.3) is closer to Ingalls's empirical result of $-0.37 a_0^3$ mm/sec than it is to the value originally obtained using free-ion wave functions for Fe²⁺ and Fe³⁺, and $-\alpha$ is greater than $0.28 a_0^3$ mm/sec, but the value of α given by (4.4) is significantly in error. This is reassuring because the assumption of ionic wave functions is supposed to be adequate for the Fe²⁺ but inadequate for Fe³⁺. We interpret the deviation from equality of the two α 's as measuring ρ_i^{cov} , the covalency contribution to the ionic charge densities. Accordingly, we assume $\alpha = -0.37 a_0^3$ mm/sec and calculate the additional charge density needed for each ion. We find

$$\rho_{2+}^{\text{cov}} = 0.56 a_0^{-3}, \quad (4.5)$$

$$\rho_{3+}^{\text{cov}} = 1.09 a_0^{-3}. \quad (4.6)$$

These densities represent approximately 10-25% of the charge densities due to an atomic 4s electron.¹⁸ The factors most significantly influencing the specific magnitudes given are the assumption of a value for α , the accuracy of the 3s-electron density estimation and the conduction-electron contribution to $|\psi_{\text{Fe}}(0)|^2$. In each case the result for the

Fe^{2+} ion is more sensitive to any change than that for the Fe^{3+} ion. Ingalls's estimate of the 3s-electron density uncertainty is about $0.1a_0^{-3}$, but perhaps there is an additional source of error from the failure of his assumption of a linear relationship between 3s charge density at the nucleus and maximum 3d charge density. Although such errors may change the numerical values of (4.5) and (4.6), it is clear that the order of magnitude is most dependent on the band-electron contribution to $|\psi_{\text{Fe}}(0)|^2$. If we had used Ingalls's value for this quantity, we would have found that covalency would have to subtract charge density from the Fe^{2+} ion, i.e., the screening by additional *d* electrons would have to outweigh the effect of transferred *s* electrons, which seems unreasonable.^{20,21}

The results (4.3)–(4.6) are in agreement with both our theoretical understanding of the role of covalency, and the experimental value of α deduced from consideration of the pressure measurements. We conclude, therefore, that our value for the band contribution to $|\psi(0)|^2$ of $4.82a_0^{-3}$ is realistic.

V. INTERPRETATION OF NEUTRON-DIFFRACTION DATA

The amplitude for elastic scattering of neutrons from a regular solid is the sum of two contributions, that due to nuclear scattering, and that due to scattering from electronic orbital and intrinsic magnetic moments.²⁴ Interference between the two types of scattering can be useful, both to produce^{2,24} polarized beams of neutrons and to measure the magnitude and sign of the magnetic scattering amplitude. The magnetic moment density is synthesized from the scattering amplitudes by a Fourier inversion summation.

For ferromagnetic iron, the scattering amplitudes have been measured and contour maps of spin

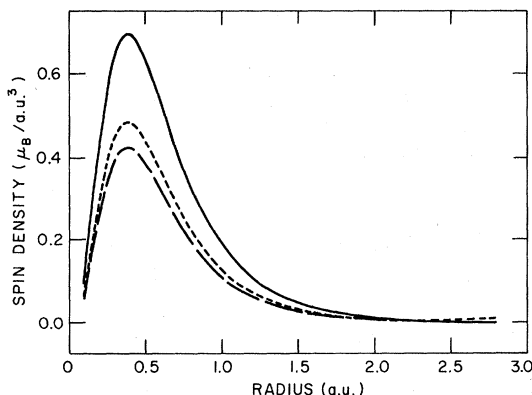


FIG. 2. The radial distribution of spin density deduced from the band wave functions. The solid line, dotted line, and dashed line are for the [100], [110], and [111] directions, respectively.

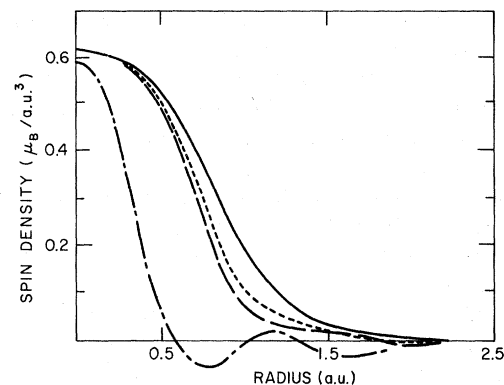


FIG. 3. The radial distribution of spin density deduced from neutron-diffraction measurement (Ref. 2). The solid line, dotted line, and dashed line are for the [100], [110], and [111] directions, respectively. The dot-dash line is the experimental resolution function.

density throughout the unit cell have been calculated.² On the theoretical side, the band-structure calculation reported in I gives us the conduction-electron wave functions from which we obtain predicted charge and spin-density distributions.

For the purposes of comparison with the experimental results, four symmetry lines were chosen along which theoretical spin densities were calculated. Twenty-five points were chosen in each of the [100], [110], and [111] directions and the results are plotted in Fig. 2 as a function of radial distance from an iron atom. The experimental results and resolution function given in Fig. 3 are taken from the graph by Shull.²

The general features of the experimental results are well reproduced by the theory. In the region $r=0.5a_0$ to about $1.7a_0$ the resolution function is sufficiently small compared with the experimental value, and it is found that the spin densities for both experiment and theory are largest for the [100] direction and smallest for the [111] direction. The magnitudes are also in satisfactory agreement. For distances greater than 2 Bohr radii, we compare directly with the results of a more detailed analysis of the experimental data.^{25,26} Figure 4 is reproduced from a schematic spin-density map given therein. Of particular interest are the regions in which the spin density is negative. Although the graphs in Fig. 3 from earlier data show the spin density going negative for all three directions considered, the analysis of Ref. 25 shows this is not the case for the [100] direction, but certainly occurs for the [110] direction. The experimental results for the [111] direction are not unequivocal, but it appears that the spin density remains positive. Just such behavior has been produced by the spin density deduced from the present band wave functions, which shows that only the [110] direction

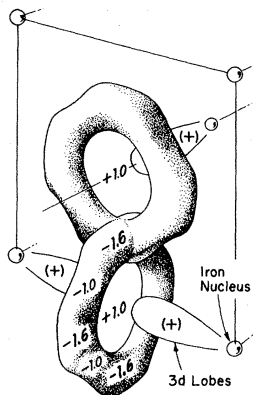


FIG. 4. The spin density for the interstitial regions deduced from neutron-diffraction measurements.²⁵ The magnetization is given in kilogauss. The magnitudes shown differ from those of Ref. 25 as a result of revised calculations by Shull.²⁶

shows slight negative spin density at large r .

As a further check, spin densities were calculated at 11 equally spaced points along a line joining the midpoint of the cube edge to the face-center position (see Fig. 4). The end points of this line are equivalent points in that each is the midpoint of a line joining second nearest neighbors. Therefore, the spin density should be symmetric about the midpoint of this line. The results are listed in Table III. It is seen that the symmetry condition is satisfied, except for a systematic error of about $0.2 \times 10^{-3} \mu_B a_0^{-3}$. Spin densities are obtained by the subtraction of two almost equal charge densities so that the computational error as a proportion of the computed result becomes more significant. It therefore appears that the systematic error represents the fact that for these small spin densities we are operating near the limit of our computational accuracy. If we allow for some additional random error, we find the spin density at the midpoint of the line under consideration to be $(-2.6 \pm 0.3) \times 10^{-3} \mu_B a_0^{-3} = -2.0 \pm 0.3$ kG, in agreement with the experimental result of -1.6 ± 0.5 kG. At the ends of the line, the theoretical result for the spin density is essentially zero. Since the spin density along the [100] line in this region is positive (see Table IV), it is possible that the result should be expressed as 0_+ . The experimental result is $+1.0 \pm 0.8$ kG.

In an attempt to extract further physical information from the neutron-diffraction data, Shull and Yamada,² and Wakoh and Yamashita¹¹ have attempted an analysis of the form factors on the basis of a crystal-field model of the conduction-electron states. Recognizing the need to incorporate the contribution due to the scattering by some residual orbital moment, Shull and Yamada write the total form factor as

$$f = 0.943 f_{\text{quenched spin}} + 0.057 f_{\text{unquenched spin}} + f_{\text{core}}, \quad (5.1)$$

with

$$f_{\text{quenched spin}} = \xi \langle j_0 \rangle + \xi (5/2\gamma - 1) A_{hk\ell} \langle j_4 \rangle + (1 - \xi) f_{4s \text{ spin}}, \quad (5.2)$$

where j_0 and j_4 are the spherical Bessel functions of order 0 and 4, respectively. The resulting fractional 4s magnetization is then

$$M_{4s}/M_t = 0.943 (1 - \xi),$$

where M_t is the total magnetic moment. The experimental group found $\gamma = 0.53 \pm 0.01$ and $\xi = 1.10$, giving a 4s magnetization of $-0.21 \mu_B/\text{atom}$. To obtain these results, they had to assume values for the Bessel function integrals based on atomic wave functions. Wakoh and Yamashita used the results of their band calculation to find $\gamma = 0.537$ and $\xi = 1.035$, yielding a 4s polarization of $-0.073 \mu_B/\text{atom}$.

Such an approach is only valid if the assumptions of the crystal-field model are justified. The results of the investigation here reported disagree with those assumptions. The evidence for that statement is as follows. Independently of the crystal-field model, it must be possible to describe the charge and spin densities of the electrons as a linear combination of the basis functions for totally symmetric representations of the cubic group. Accordingly, the spin density was written as²⁷

$$\rho = \rho_0 Y_0^c + \rho_4 Y_4^c + \rho_6 Y_6^c, \quad (5.3)$$

where $Y_0^c = 1/(4\pi)^{1/2}$,

$$\begin{aligned} Y_4^c &= Y_4^0 + \frac{1}{2}(10)^{1/2} (Y_4^4 + Y_4^{-4}) \\ &= (15/4\pi^{1/2}) (x^4 + y^4 + z^4 - \frac{3}{5}r_4)/r^4, \\ Y_6^c &= Y_6^0 - \frac{1}{2}(14)^{1/2} (Y_6^4 + Y_6^{-4}) \\ &= 14(13/4\pi)^{1/2} \left\{ \frac{15}{14}r^6 - [x^6 + y^6 + z^6 + \frac{15}{4}(x^4y^2 + x^2y^4 + x^2z^4 + x^4z^2 + y^2z^4 + y^4z^2)] \right\} / r^6, \end{aligned}$$

where Y_i^m is the usual spherical harmonics. The coefficients ρ_0 , ρ_4 , and ρ_6 were obtained by fitting

TABLE III. Spin density along a line joining the face-center position to the midpoint of a cube edge.

Displacement from face center	Spin density ($\mu_B a_0^{-3} \times 10^{-3}$)
0.0 (face center)	-0.14
0.1	-0.42
0.2	-1.11
0.3	-1.89
0.4	-2.45
0.5	-2.63
0.6	-2.39
0.7	-1.77
0.8	-0.94
0.9	-0.20
1.0 (midpoint of cube edge)	+0.14

TABLE IV. Spin densities in three directions and their analysis into Kubic harmonics. ρ_0 , ρ_4 , and ρ_6 are defined in Eq. (5.3). The last column gives the ratio of the coefficients of Y_4^2 from the spin and charge densities.

Radius (a.u.)	[100]	[110]	[111]	ρ_0	ρ_4	$\rho_6 (10^2)$	$\rho_4^{\text{spin}}/\rho_4^{\text{charge}}$
0.1	0.0974	0.0668	0.0576	0.259	0.0283	0.022	-2.34
0.2	0.4215	0.2954	0.2578	1.141	0.1167	0.104	-5.06
0.24	0.5335	0.3738	0.3263	1.444	0.1476	0.133	-5.88
0.28	0.6164	0.4316	0.3768	1.667	0.1707	0.155	-6.38
0.32	0.6688	0.4680	0.4084	1.808	0.1855	0.169	-6.65
0.36	0.6936	0.4851	0.4232	1.874	0.1927	0.175	-6.78
0.40	0.6956	0.4862	0.4240	1.879	0.1936	0.176	-6.84
0.44	0.6800	0.4749	0.4140	1.836	0.1896	0.172	-6.89
0.48	0.6516	0.4546	0.3961	1.758	0.1821	0.164	-6.94
0.52	0.6146	0.4284	0.3731	1.657	0.1721	0.154	-7.01
0.56	0.5725	0.3987	0.3469	1.542	0.1608	0.142	-7.09
0.60	0.5281	0.3673	0.3194	1.421	0.1487	0.130	-7.19
0.68	0.4395	0.3049	0.2646	1.180	0.1246	0.106	-7.43
0.80	0.3228	0.2228	0.1927	0.864	0.0926	0.074	-7.83
1.2	0.1096	0.0739	0.0627	0.288	0.0333	0.017	-5.96
1.6	0.0393	0.0258	0.0218	0.102	0.0125	0.011	-1.90
2	0.0137	0.0081	0.0083	0.336	0.0033	0.042	-0.36
2.1	0.0090	0.0056	0.0069	0.244	0.0018	0.057	-0.18
2.2	0.0061	0.0036	0.0060	0.174	0.0005	0.075	-0.04
2.3	0.0038	0.0020	0.0055	0.120	-0.0007	0.097	0.06
2.4	0.0021	0.0007	0.0056	0.008	-0.0018	0.123	0.14
2.5	0.0009	-0.0003	0.0061	0.006	-0.0028	0.154	0.20
2.6	0.0002	-0.0010	0.0071	0.005	-0.0038	0.194	0.24
2.7	0.0000	-0.0014	0.0086	0.006	-0.0048	0.242	0.27
2.8	0.0003	-0.0017	0.0108	0.007	-0.0058	0.302	0.29

the spin densities calculated for the three directions [100], [110], and [111] to the expression (5.3) and they are given in Table IV. It is to be noticed that ρ_6 is everywhere small. A significant feature is that the only coefficient that changes sign is ρ_4 for the larger distances. Since ρ_4 derives its contribution predominantly from d -like states, this necessarily implies a spin dependence of the radial part of the d -electron wave functions, and so expectation values of j_0 and j_4 with respect to the d wave function are spin dependent. Equation (5.2), however, is constructed on the assumption that the entire spin density is due solely to a population differential between the two sets of spin states. In the last column of Table IV we list the ratio $\rho_4^{\text{spin}}/\rho_4^{\text{charge}}$ as a function of radius. For a crystal-field model this quantity should be constant, at least where interatom overlap is small (i.e., ρ_6 small). From $r=0.2a_0$ to $r=0.8a_0$ the magnitude of this ratio increases by 50% and is then followed by a precipitous drop, reflecting the over-all decline in the spin density for radii greater than $1.0a_0$. De Cicco and Kitz²⁸ examined their charge and spin densities, which were proportional to those of Wakoh and Yamashita, and both of these also showed marked radial dependence of the ratio $\rho_4^{\text{spin}}/\rho_4^{\text{charge}}$.

It must be remembered that any polarization of the 4s states would be reflected in ρ_0 only, so that the decline of ρ_4^{spin} with respect to ρ_4^{charge} shows that

the decrease in spin density in the outer regions of an atomic site, leading to regions of negative polarization, are not adequately explained by a negative polarization of the 4s states. This does not rule out the possibility of some negative 4s polarization, but it does considerably diminish the usefulness of the crystal-field model in the interpretation of the neutron-diffraction data. This undoubtedly comes about by the failure of the crystal-field wave functions and populations to adequately represent band wave functions whose radial character, symmetry properties, and resulting populations change with position in the BZ. For example, De Cicco and Kitz examined the radial character of their d wave functions as a function of energy and found typical variations of about 5%.

Although the crystal-field model fails, it is possible to retain some of its features for a qualitative explanation of the spin-density distribution. In some regions of the BZ there are some majority-band states occupied while the corresponding minority-band states are empty. If, over-all the charge clouds for such states tend to point in the [100] direction, the population differential alone will ensure that the spin density is always positive in this direction. Suppose now the states which are preferentially oriented in the [110] direction are predominantly spin paired. In that case the radial part of the wave function can decide the spin-density behavior and can provide the regions of nega-

tive spin density. No detailed analysis of the angular character of the wave functions found in I was attempted, but by comparison with Wood's band structure²⁹ the symmetry classifications could be determined, and it is readily seen that the necessary conditions are met for the above qualitative explanation of the spin-density distribution.

The band calculation thus appears to be well capable of reproducing the experimental spin densities. The regions of negative polarization appear to be caused by a spin dependence of the radial part of the *d*-electron wave function. No evidence was found that the 4s electrons are antipolarized, but neither was any found to the contrary. However, the analysis which has led others to conclude that the 4s electrons are antipolarized has been found faulty.

VI. HYPERFINE FIELD

Before presenting our results we will review the experimental and theoretical situations with respect to the hyperfine field.

In a series of experiments on ferromagnetic iron using the Mössbauer effect, Hanna and co-workers demonstrated that (a) the direction of the nuclear magnetic moment is strongly correlated with the direction of magnetic polarization of the electronic system,³⁰ (b) the magnitude of the effective field causing the nuclear orientation is 333 kOe,³¹ and (c) the effective field has a negative sign.³² Subsequently, it has become apparent³³ that this behavior is characteristic of the transition metals and their alloys. Although the sign of the hyperfine field was unexpected,³⁴ it was immediately recognized, both by the original experimental group and by Goodings and Heine,³⁵ in the first attempt at a theoretical explanation of the negative sign that a potential source of a large negative field was the core electrons. The Hamiltonian for the interaction between the nuclear magnetic moment and an electron spin is

$$H_c = \frac{16}{3} \pi \gamma_e \gamma_n \hbar^2 \sum_i \vec{I} \cdot \vec{S}_i \delta(\vec{r}_i) ,$$

where γ_e and γ_n are the electron and nuclear magnetogyric ratios, \vec{I} and \vec{S}_i are the nuclear and electron spins, respectively. This is called the "Fermi contact interaction." Matrix elements of H_c involving a non-*s*-like state are zero because of the δ function in the Hamiltonian. If states of both spin polarity are occupied, then the matrix elements can be nonzero only if the magnitude of the wave functions at the nucleus are spin dependent. A mechanism which brings about this spin dependence, ECP, was originally proposed by Sternheimer³⁶ in his investigation of hyperfine fields of atoms and is based on the fact that in the Hartree-Fock (HF) equations for a given state there exist exchange terms with all other states of the same spin, but not with states of opposite spin. Thus, if there are any unpaired spins in the system, the core-state wave functions will be spin dependent. This basic mechanism has been applied successfully to an explanation of hyperfine fields and other magnetic properties in a wide variety of substances.³⁷

In Table V are listed the contributions to the hyperfine field in iron as calculated by previous investigators. The contribution from 4s states that Goodings and Heine used is from an estimate by Marshall³⁴ on the basis of Pauli paramagnetism of the conduction electrons due to an effective magnetic field via the exchange interaction with the magnetic *d* electrons. In this model, the 4s-state polarization is certainly positive and, assuming no significant contribution from spin dependence of the wave functions of states occupied by electrons of both spins, the contribution to the hyperfine field is certainly positive. Two entries are listed for these workers for the ECP contribution. The first is on the basis of a calculation for atomic iron $3d^6 4s^2$ configuration. For the second, the *d*-state wave functions were artificially expanded by 5% at the maxima and 10% in the tails in order to simulate expanded wave functions which were believed³⁸ to be appropriate for the metal. It is apparent from the last column of Table V that they were unable to achieve agreement with experiment without

TABLE V. Hyperfine field in kilogauss as calculated by various authors.

	Core-electron contribution	Band-electron contribution			Total hyperfine field
		Direct	Hybridization	Total	
Goodings and Heine (Ref. 35)					
Atomic $3d^6 4s^2$	- 355			70-250	- 285 to (- 105)
Expanded 3d functions	- 420			70-250	- 350 to (- 170)
Freeman and Watson (Ref. 39)					
Atomic $3d^6 4s^2$	- 320			200	- 120
Atomic $3d^8$	- 350			200	- 150
Muto, Kobayasi, and Hayakawa (Ref. 40)	- 1145	656	150	806	- 339
Wakoh and Yamashita (Ref. 11)	- 356			- 52	- 408

the expanded functions, and that some agreement was obtained by using those functions.

In order to pursue the impact of the expanded wave functions and also to incorporate the belief that the electronic configuration of the metal differed from that of the free atom, Freeman and Watson³⁹ repeated Goodings and Heine's calculation and also did a similar calculation for the $3d^8$ configuration. The results for the $3d^6 4s^2$ configurations by both groups of authors are in substantial agreement. Watson and Freeman point out that, although the $3d^8$ configuration does give an expanded charge density, the spin density, which is the relevant factor, is not significantly changed and only decreases slightly the discrepancy between the theory and experiment. They further point out that the artificially expanded $3d^6 4s^2$ configuration gives a spin density in disagreement with experiment. They further add that it is typical of unrestricted Hartree-Fock (UHF) calculations to overestimate the magnitude of the ECP contribution. Thus Freeman and Watson discredit the view that the negative hyperfine field is adequately explained on the basis of an ECP contribution large enough to offset a positive contribution from conduction electrons. The question of the polarization of the $4s$ electrons is therefore clearly relevant, and an estimate of environmental effects on the ECP contribution is also necessary.

Two treatments of the iron hyperfine problem using band-theory approaches have been given previously and the results are given in Table V. The first by Muto, Kobayasi, and Hayakawa⁴⁰ produces a total hyperfine field in agreement with experiment, but only by virtue of a judicious and arbitrary choice of a hybridization contribution equal to almost half the magnitude of the final result. It is somewhat disquieting that their individual contributions are significantly larger than the estimates by both of the preceding sets of authors. Additionally, Muto and co-workers found it necessary to introduce rather arbitrarily chosen $3d$ wave functions, again to simulate a spread-out charge density. Further, the perturbation theory used by these authors to calculate ECP effects is inaccurate. For example, they use for the perturbed core states the wave functions

$$\Phi'_{ns} = \Phi_{ns}^{*0} + \sum_{n'} \Phi_{n's}^{*0} \frac{\langle n's\uparrow | A | ns\uparrow \rangle}{\epsilon_{ns} - \epsilon_{n's}} + \sum_{\vec{k}} \Phi_{4s\vec{k}}^{*0} \frac{\langle \vec{s}\vec{k}\uparrow | A | ns\uparrow \rangle}{\epsilon_{ns} - \epsilon_{4s\vec{k}}},$$

where A is an effective exchange operator.⁴⁰ This form of perturbation theory would require a careful choice of one-electron excited states so that they form a complete set. This would entail different excited states for different cores, which have not been employed. Also, it requires a detailed knowledge of both core and band-electron energies. Thus this calculation serves only to

reinforce the view that the charge and spin densities of the $3d$ electrons must be carefully treated, and reaffirms that a large negative contribution comes from ECP, but it does not quantitatively explain the magnitude of iron's hyperfine field.

The second band-theory treatment was by Wakoh and Yamashita.¹¹ The contribution from core states was found on the basis of the UHF calculation for the core states. The contribution from the conduction electrons through the contact interaction was determined directly from the wave functions of the occupied states at 14 symmetry points in $\frac{1}{48}$ of the BZ. They claim a net polarization of the $4s$ states of -0.011 electrons, contributing -52 kG to the hyperfine field. They state that the contribution comes solely from the unpaired $4s$ electrons, and there is no contribution from spin dependence of the $4s$ wave function. This result appears to conflict with the band structure as given by them, in which all minority states lie above the corresponding majority states, necessarily implying that no matter which minority states are occupied, the corresponding majority states are also occupied. That is, the inference from the band structure is of a positive contribution to the $4s$ population and to the hyperfine field. Hybridization of $4s$ and $3d$ states can produce a negative contribution to polarization, and the influence of this will be examined below.

From a perturbation-theory point of view, the hyperfine interaction energy of core electrons may be regarded as a second-order energy, because it consists of two small perturbations, namely, exchange polarization of the core electrons and the contact interaction. Therefore, the energy may be calculated either from the expectation value of the contact Hamiltonian using spin-polarized wave functions [exchange polarized (EP)] or from the expectation value of the exchange interaction using wave functions perturbed by the contact interaction [moment polarized (MP)]; these two methods have been shown to be equivalent.⁴¹ For the present calculation the MP method was used; the MP wave functions were supplied by Ikenberry⁴² for the iron $3d^7 4s^{0.5} 4s^{0.5}$ configuration, which configuration is very close to that found in the metal.¹¹ The method used to obtain these functions was that of Dalgarno⁴³ with a local approximation to the HF Hamiltonian. After orthogonalizing the MP functions to the core states, the following integral has to be calculated for each occupied-band wave function:

$$\int \psi_{\text{band}}^*(1) \psi_{\text{core}}(1) \frac{1}{r_{12}} \psi_{\text{core}}^{*\text{MP}}(2) \psi_{\text{band}}(2) d\tau_1 d\tau_2.$$

The basic techniques used to calculate these integrals were essentially the same as those used to calculate normal exchange integrals as described

in I. Using the basis functions described in Sec. II, the matrix elements were calculated, the sum over core states performed, and the linear combinations appropriate to the band wave functions formed. Finally, the sum over occupied states is calculated. Because we performed the sum over core states at an intermediate stage (to save computer time) we are not able to list contributions from individual core shells.

The total core contribution was calculated to be -447 kG. The value for 2.2 unpaired atomic d electrons with radial wave functions appropriate for the $3d^74s$ configuration was -404 kG. Thus, the influence of the itinerancy of the wave function is found to be an increase in the magnitude of the hyperfine field by about 10%.

The contribution of -447 kG is somewhat higher than Wakoh and Yamashita's estimate¹¹ of -356 kG and Freeman and Watson's estimate³⁹ of -340 kG, both based on UHF calculations for the core electrons. A previous exploration⁴⁴ of computational aspects of the perturbation problem for core electrons has shown that the magnitude of the ECP contribution should be decreased by about 10% to correct for the use of Dalgarno's formalism and the use of a local operator for the HF Hamiltonian, and to incorporate an indirect spin polarization through a $2p$ and $3p$ spin density. Thus the contribution from the core states comes to about -400 kG, still more than 10% higher than Freeman and Watson's original estimate.

The band wave functions calculated for the conduction electrons already incorporate spin polarization, so that no perturbation treatment is necessary for them. The expectation value of the hyperfine Hamiltonian gives directly a band contribution of 33.1 kG. When added to the core contribution, the total hyperfine field is -367 kG which is about 35 kG more negative than the experimental result. The deficiency could, perhaps, be attributed to correlation effects associated with core electrons.

It is well to emphasize the two physical results which emerge from the present calculation and help resolve the doubts originally raised by Freeman and Watson regarding the efficacy of the ECP mechanism. They are (a) an increased core contribution of about 10% due to environmental effects on the polarizing d wave functions; (b) a greatly decreased positive contribution from the band.

To further elucidate the band contribution, the hyperfine field of the unpaired electrons only was calculated. It was $+177$ kG which is about the same size Watson and Freeman originally estimated. The paired band electrons then contribute -144 kG. It was not possible to separate this into spin polarization and hybridization components, but the magnitude is certainly too large to be accounted for by a spin dependence of the radial wave function

through exchange polarization, so hybridization is probably the dominant influence. Qualitative insight into this mechanism is gained by consideration of the ΓH line, where the s bands hybridize with the d bands sooner for the majority spin than for the minority spin, because, for the former, the d bands are separated from the s bands by larger energies than those for the latter. This means the s character can be transferred faster to a higher-lying unpaired band for the majority spin than for the minority spin.

The band contribution was also calculated for the case where the magnetic moment was 2.06 μ_B /atom, and this is also listed in Table II. In this case the band hyperfine contribution rose to $+57.7$. Again this illustrates the influence of hybridization. As the magnetic moment is decreased by lowering the minority-spin bands with respect to the majority-spin bands, the minority bands hybridize more strongly and thus lower minority s charge density, increasing the net band contribution to the hyperfine field. If some of the magnetic moment of iron is due to orbital moments (De Cicco and Kitz⁴⁵ estimate 0.08 μ_B /atom), then the spin moment would be smaller than that used throughout this calculation, and a larger band contribution lying between 33.1 and 57.7 would result, increasing the agreement between theory and experiment.

The positive-band contribution found here is in contradistinction to the result of Wakoh and Yamashita who find a negative contribution of about the same size as was found here. The present result is more in accord with what one might expect on the basis of an atomic model, and in fact, if Watson and Freeman³⁹ had taken into account the role of hybridization in diminishing (but not reversing, as Wakoh and Yamashita¹¹ find) the polarization of the $4s$ states, they would have had an acceptable model for the hyperfine field.

On the basis of the present investigation it is concluded that the $4s$ electrons are positively polarized. Experimentally, it is known that the hyperfine field induced by nearest-neighbor and next-nearest-neighbor atoms is negative.⁴⁶ Consider the coupling of a d electron (d_A) on site A with a d electron (d_B) on site B through their mutual interaction with the $4s$ electrons [Ruderman-Kittel-Kasuya-Yosida (RKKY) mechanism⁴⁷]. We consider only the change s_A or s_B in the s spin density caused by the d - s interaction. If d_A is polarized \uparrow , from the present work we conclude s_A is polarized \uparrow , but from the experimental work we know that s_B is polarized \downarrow . Then again from the present work, it is most energetically favorable for d_B to be polarized with the same sense as s_B , that is \downarrow . Thus the RKKY mechanism favors d states on neighboring sites to be antipolarized,

that is, antiferromagnetic coupling which opposes the tendency to ferromagnetism. This has previously been noted by Overhauser and Stearns.⁴⁸ Consideration of the origin of the ferromagnetism has been given in I.

Finally, we return to the question of the pressure dependence of the hyperfine field. Recalling that the band effect on the ECP was to increase its magnitude by about 10%, Anderson's³ assumption that the *d* bands are so compact that pressure should have little effect is suspect. The following model is, therefore, suggested to explain the negative trend with pressure of the hyperfine field per spin: There is competition between an increased negative core-polarization contribution due to pressure-widened *d* bands and a positive contribution from the *s*-like states. The experimental value for the pressure coefficient of the hyperfine field per spin is found to be much smaller for iron than for cobalt and nickel,³ suggesting the more markedly competitive nature of these processes in iron. That the *d* charge density in a transition metal can be compressed significantly by application of pressure has also been demonstrated recently in an experimental study of the pressure dependence of the Knight shift in vanadium.⁴⁹

VII. DISCUSSION

In this paper we have studied the wave functions produced by a recent band calculation for the ferromagnetic state of iron. The properties treated were those which provide a direct measure of the wave functions, namely, charge and spin densities, both in the nuclear region and throughout the rest of the unit cell. The predictions from the wave functions were, generally, in excellent agreement with the corresponding experimentally known quantities. Having demonstrated the reliability of the wave functions, we then used them to show that the interpretation of previous data in favor of a negative polarization of the 4s electrons is not acceptable. Specifically, we showed that the use of a crystal-field model to interpret neutron-diffraction data is not justified, and that the core-polarization contribution to the hyperfine field is sensitive to the environment of the *d* electrons and therefore to pressure, which then invalidates a discussion of the pressure dependence of the hyperfine field on the basis of *s* states alone.

The affirmative evidence we presented in favor of a positive polarization of the 4s states was that of a positive contribution to the hyperfine field from the conduction electrons. The strength of this evidence lies in the accuracy of the wave functions. Of course, it is of particular importance that the calculated total hyperfine field be in agreement with experiment and that unconsidered contributions be small. The major omission was

a consideration of the contributions to the contact interaction arising from the dynamic correlation of core states with one another and with the 4s electrons, and the correlation between 3*d* and 4s states. An exact treatment of these effects is beyond present computational capabilities, but we can gain some insight from some many-body treatments of atoms.

Two many-body formalisms have been used extensively in atoms: the Brueckner-Goldstone^{50,51} and the Bethe-Goldstone⁵² techniques; where these have been applied to the same systems, excellent agreement with each other, as well as with experiment, has been achieved. Moreover, it is possible to identify in the Brueckner-Goldstone diagram expansion, terms which correspond to the ECP procedure⁵¹ (EP or MP), and to calculate such contributions. Approximate agreement is achieved between the results of the diagrammatic procedure and the MP results and it is believed⁴² that the difference is accounted for by the use of the local-exchange approximations in the numerical procedures of the MP and EP methods. This gives confidence in the concept of the HF perturbation process, although not necessarily implying that the result of the perturbation process will always be in agreement with experiment.

From an analysis of the results that have been obtained already for hyperfine effects in atoms through the use of Brueckner-Goldstone many-body procedure,⁵¹ one can make some reasonably general observations concerning the role and importance of correlation effects with respect to hyperfine interactions. (a) Correlation effects are always important; however, they have determining importance when core-polarization contributions suffer considerable mutual cancellation. (b) The correlation among electrons within an incomplete shell of given angular symmetry contributes nothing to the hyperfine field. (c) If there exists an unoccupied *s* state almost degenerate with an unpaired non-*s* state, correlation effects should be quite important, for example, the Li 2P configuration where the occupied $2p$ state is nearly degenerate with the unoccupied $2s$ state. (d) If, for the non-*s* state in question, there exists an occupied *s* state such that both have large amplitudes over a significant common volume, their mutual correlation will be important. A particularly remarkable example of this situation is the case of the phosphorous atom where a large contribution comes from the $3p$ - $3s$ correlation.

For atomic iron ($3d^6 4s^2$) the 1*s*, 2*s*, and 3*s* ECP contributions are almost completely cancelled by the 4*s* contribution, and correlation contributions should be the determining factor. In particular, by rule (d) the 3*d*-4*s* correlation could be important. In going to the metal, the configuration changes to

$3d^7 4s$ and the $4s$ wave function becomes more diffuse, making the $4s$ (band) contribution less effective than in the atom. From our calculation it is seen that there is no marked cancellation between the $4s$ -band contribution and that of the $1s$, $2s$, and $3s$ states. Observation (a) then indicates that correlation effects should no longer be of crucial importance. Also, because s states in the metal correspond to rapidly rising bands, there will be only small regions of the BZ where they cross the relatively flat d bands, so that the provisions of rule (c) should not be operative to any great extent. Additionally, rule (d), which can be effective for the atom, may be diluted for the metal because of the more diffuse $4s$ wave function.

It should be emphasized that no Brueckner-Goldstone treatment of a metal has yet been given, so that the above suggestions regarding the metal are merely plausibility arguments. They are, however, our best guide, and on that basis it seems

reasonable to assume that an ECP calculation without correlation effects should give quite reliable results. In conclusion then, we have reason to feel confident about our result that the band $4s$ states are positively polarized.

This conclusion for iron is not easily extrapolated to cobalt or nickel. Exchange polarization and hybridization influences are competitive, and both diminish with diminishing net magnetic moment. Which one will dominate could easily be determined by factors such as the crystal structure.

ACKNOWLEDGMENTS

We are grateful for the cooperation and assistance given to us by Dr. M. Garber, Director of the Computing Center, University of California, Riverside. The iron MP functions were supplied by Dr. Dennis Ikenberry, which we gratefully acknowledge. We thank Professor C. G. Shull for correspondence regarding Fig. 4.

*This work was supported in part by a National Science Foundation Grant at The University of California, Riverside, Calif. 92502.

¹N. F. Mott, *Adv. Phys.* 13, 325 (1964); P. W. Anderson and A. M. Clogston, *Bull. Am. Phys. Soc.* 6, 124 (1961).

²C. G. Shull and Y. Yamada, *J. Phys. Soc. Japan Suppl.* 17, 1 (1962); C. G. Shull, *Verband Deutscher Physikalischer Gesellschaften. Physikertagung. Hauptvertrage* (Verlag, Baden, West Germany, 1962).

³D. H. Anderson, *Solid State Commun.* 4, 189 (1966).

⁴P. E. Mijnarens and L. Hambro, *Phys. Letters* 10, 272 (1964); V. L. Sedov, L. V. Solamatina, and L. A. Kondrashova, *Zh. Eksperim. i Teor. Fiz.* 54, 1626 (1968) [Soviet Phys. *JETP* 27, 870 (1968)]; T. W. Mihalisin and R. D. Parks, *Phys. Letters* 13, 339 (1964).

⁵K. J. Duff and T. P. Das, *Phys. Rev. B* 3, 192 (1971), hereafter called I.

⁶S. Berko and J. Zukerman, *Phys. Rev. Letters* 13, 339 (1964); T. W. Mihalisin and R. D. Parks, *ibid.* 18, 210 (1967); *Solid State Commun.* 7, 33 (1964); V. L. Sedov, *Usp. Fiz. Nauk USSR* 94, 417 (1968) [Soviet Phys. *Usp.* 11, 163 (1968)].

⁷S. Berko and A. P. Mills, *Bull. Am. Phys. Soc.* 15, 270 (1970).

⁸R. V. Pound, G. B. Benedek, and R. Drever, *Phys. Rev. Letters* 7, 405 (1961); D. N. Pipkorn, C. K. Edge, P. Debrunner, G. De Pasquali, H. G. Drickamer, and H. Frauenfelder, *Phys. Rev.* 135, A1604 (1964); W. H. Southwell, D. L. Decker, and H. P. Vanfleet, *ibid.* 171, 354 (1968); M. Nicol and G. Jura, *Science* 141, 1035 (1963); J. D. Litster and G. B. Benedek, *J. Appl. Phys.* 34, 688 (1963).

⁹L. Hedin, *Phys. Rev.* 139, A796 (1965).

¹⁰J. Hubbard, *Proc. Roy. Soc. (London)* A276, 238 (1963); A277, 237 (1964); A281, 401 (1964).

¹¹S. Wakoh and J. Yamashita, *J. Phys. Soc. Japan* 21, 1712 (1966); 25, 1272 (1968).

¹²B. W. Batterman, D. R. Chipman, and J. J. De Marco, *Phys. Rev.* 122, 68 (1961).

¹³B. W. Batterman, *Phys. Rev. Letters* 2, 47 (1959).

¹⁴P. M. Raccah, R. N. Euwema, D. J. Stukel, and T. C. Collins, *Phys. Rev. B* 1, 756 (1970).

¹⁵F. J. Arlinghaus, *Phys. Rev.* 153, 743 (1967).

¹⁶R. Ingalls, *Phys. Rev.* 155, 157 (1967).

¹⁷H. G. Drickamer, R. W. Vaughan, and A. R. Champion, *Accounts Chem. Res.* 2, 40 (1969).

¹⁸L. R. Walker, G. K. Wertheim, and V. Jaccarino, *Phys. Rev. Letters* 6, 98 (1961).

¹⁹R. E. Watson, *Solid State and Molecular Theory Group, MIT Technical Report No. 12*, 1959 (unpublished).

²⁰V. I. Gol'danski, *Proceedings of the Dubna Conference on the Mössbauer Effect* (Consultants Bureau Enterprises, New York, 1963).

²¹J. Danon, *Application of the Mössbauer Effect in Chemistry and Solid State Physics* (International Atomic Energy Agency, Vienna, 1966).

²²E. Simanek and Z. Sroubek, *Phys. Rev.* 163, 275 (1967); E. Simanek and A. Y. C. Wong, *ibid.* 166, 348 (1968).

²³J. A. Moyzis, Jr. and H. G. Drickamer, *Phys. Rev.* 171, 389 (1968).

²⁴A review of the theory of nuclear and magnetic scattering of neutrons has been given by W. M. Lomer and G. G. Low, in *Thermal Neutron Scattering*, edited by P. A. Egelstaff (Academic, New York, 1965).

²⁵C. G. Shull and H. A. Mook, *Phys. Rev. Letters* 16, 184 (1965).

²⁶C. G. Shull (private communication).

²⁷F. C. von der Lage and H. A. Bethe, *Phys. Rev.* 92, 1129 (1953).

²⁸P. De Cicco and A. Kitz, *Quarterly Progress Report, Solid State and Molecular Theory Group, MIT* 62, 13 (1966); 63, 2 (1967).

²⁹J. H. Wood, *Phys. Rev.* 126, 517 (1962).

³⁰G. J. Perlow, S. S. Hanna, M. Hamermesh, C. Littlejohn, D. H. Vincent, R. S. Preston, and J. Heberle, *Phys. Rev. Letters* 4, 74 (1960).

³¹S. S. Hanna, J. Heberle, C. Littlejohn, G. J. Perlow, R. S. Preston, and D. H. Vincent, *Phys. Rev. Letters* 4, 177 (1960).

³²S. S. Hanna, J. Heberle, G. J. Perlow, R. S.

Preston, and D. H. Vincent, Phys. Rev. Letters 4, 513 (1960).
³³See Table V given by A. J. Freeman and Richard E. Watson, in *Magnetism*, Vol. IIa, edited by George T. Rado and Harry Suhl (Academic, New York, 1965); many additional references are quoted therein.
³⁴W. Marshall, Phys. Rev. 110, 1280 (1958).
³⁵D. A. Goodings and V. Heine, Phys. Rev. Letters 5, 370 (1960).
³⁶R. M. Sternheimer, Phys. Rev. 86, 316 (1952).
³⁷R. E. Watson and A. J. Freeman, Phys. Rev. 123, 2027 (1961); and references cited therein.
³⁸Conyers Herring, J. Appl. Phys. 31, 3S (1960).
³⁹A. J. Freeman and R. E. Watson, Phys. Rev. Letters 5, 498 (1960); R. E. Watson and A. J. Freeman, J. Appl. Phys. Suppl. 32, 118 (1961).
⁴⁰Toshinosuke Muto, Syoiti Kobayasi, and Hiroko Hayakawa, J. Phys. Soc. Japan 20, 388 (1962).
⁴¹G. Gaspari, Wei Mei Shyu, and T. P. Das, Phys. Rev. 134, A852 (1964).
⁴²D. Ikenberry (private communication).
⁴³A. Dalgarno, Advan. Phys. 11, 281 (1962); Proc. Roy. Soc. (London) A251, 282 (1959).
⁴⁴K. J. Duff and T. P. Das [Phys. Rev. 168, 43 (1968)] report a calculation for Fe³⁺ which is qualitatively similar to the present system. Although the EP method was used, a subsequent calculation by D. Ikenberry

(private communication) using the MP Dalgarno method gave almost exact agreement, shell by shell, with the EP calculation. The estimates of the corrections discussed for the EP method should therefore apply to the present MP calculation.

⁴⁵P. D. De Cicco and A. Kitz, Phys. Rev. 162, 486 (1967).
⁴⁶Mary Beth Stearns, Phys. Rev. 147, 439 (1966).
⁴⁷M. A. Ruderman and C. Kittel, Phys. Rev. 96, 99 (1954); T. Kasuya, Progr. Theoret. Phys. (Kyoto) 16, 45 (1956); K. Yosida, Phys. Rev. 106, 893 (1957).
⁴⁸A. W. Overhauser and M. B. Stearns, Phys. Rev. Letters 13, 316 (1964).
⁴⁹T. Kushida and J. C. Murphy, Phys. Rev. 178, 433 (1969).
⁵⁰H. P. Kelly, Phys. Rev. 131, 684 (1963); 136, B896 (1964); 144, 39 (1966).
⁵¹E. S. Chang, R. T. Pu, and T. P. Das, Phys. Rev. 174, 1 (1968); H. P. Kelly, *ibid.* 173, 142 (1968); 180, 55 (1969); N. C. Dutta, C. Matsubara, R. T. Pu, and T. P. Das, Phys. Rev. Letters 21, 1139 (1968); Phys. Rev. 177, 33 (1969); J. D. Lyons, R. T. Pu, and T. P. Das, *ibid.* 178, 103 (1969); 186, 266 (1969); T. Lee, N. C. Dutta, and T. P. Das, Phys. Rev. A 1, 995 (1970).
⁵²R. K. Nesbet, Phys. Rev. 155, 51 (1967); 155, 56 (1967); 175, 2 (1968).

Dynamics of Ferroelectric Rochelle Salt

B. Žeks, G. C. Shukla, and R. Blinc

Institute "J. Stefan," University of Ljubljana, Ljubljana, Yugoslavia

(Received 3 August 1970)

A quantum theory of ferroelectricity in Rochelle salt is developed which is an extension of the two-sublattice model of Mitsui. The isotope effects on deuteration are explained in a natural way, and the spontaneous polarization, the polarization of the two sublattices, and the dielectric constant are obtained as functions of temperature. The dynamics of the system is investigated for the case of deuterated Rochelle salt and is found to exhibit a two-mode relaxational behavior. The correlation time of one of these two modes is proportional to the static dielectric constant and thus exhibits a critical slowing-down on approaching the two Curie temperatures in agreement with the experimental data.

I. INTRODUCTION

Though Rochelle salt has been the first ferroelectric crystal to be discovered,¹ it is still not understood very well from a microscopic point of view. The shifts of the upper Curie point towards higher temperatures and of the lower towards lower temperatures on deuteration demonstrate the role of the hydrogen atoms in its ferroelectric behavior, but no theoretical explanation of these isotope shifts which increase the ferroelectric range by about 40% has been proposed so far. Whereas the lattice dynamics of both hydrogen-bonded "order-disorder"-type ferroelectrics and of "displacive" ionic ferroelectrics seems to be basically well under-

stood, this is not the case for Rochelle salt.

It is the purpose of this note to present a quantum theory of ferroelectricity in Rochelle salt which is capable of describing the isotope effects on deuteration as well as the dynamics of dipole moment reversal in this crystal. The theory is essentially a quantum extension of Mitsui's model² along the lines used^{3, 4} to describe quantum effects in KH₂PO₄-type ferroelectrics. It is based on recent neutron-diffraction⁵ and magnetic-resonance studies^{6, 7} and assumes that the ferroelectric dipoles move in asymmetric double-well crystalline potentials and form two interpenetrating sublattices² (Fig. 1). The asymmetric double-well potentials for the two sublattices are mirror images of each other, and